The effectiveness of lidar remote sensing for monitoring forest cover attributes and landscape restoration

Almeida, D.R.A.; Stark, S.C.; Chazdon, R.; Nelson, B.W.; Cesar, R.G.; Meli, P.; Gorgens, E.B.; Duarte, M.M.; Valbuena, R.; Moreno, V.S.; Mendes, A.F.; Amazonas, N.; Gonçalves, N.B.; Silva, C.A.; Schietti, J.; Brancalion, P.H.S.

Forest Ecology and Management

DOI:
10.1016/j.foreco.2019.02.002

Published: 15/04/2019

Peer reviewed version

The effectiveness of lidar remote sensing for monitoring forest cover attributes and landscape restoration

Almeida, D. R. A.[a]; Stark, S. C.[b]; Chazdon, R[c]; Nelson, B. W.[d;] Cesar, R. G.[a]; Meli, P.[a]; Gorgens, E. B.[e]; Duarte, M. M.[a]; Valbuena, R.[f,g]; Moreno, V. S.[a]; Mendes, A. F.[a]; Amazonas, N.[a]; Gonçalves, N. B.[d]; Silva, C. A.[h]; Schietti, J.[d]; Brancalion, P. H. S.[a]

[a] Department of Forest Sciences, "Luiz de Queiroz" College of Agriculture, University of São Paulo (USP/ESALQ), Piracicaba, SP, Brazil.
[b] Department of Forestry, Michigan State University, East Lansing, MI, USA.
[c] Department of Ecology & Evolutionary Biology, University of Connecticut, Storrs, CT, USA.
[d] National Institute for Amazon Research (INPA), Manaus, AM, Brazil.
[e] Department of Forestry, Federal University of Vales do Jequitinhonha e Mucuri (UFVJM), Diamantina, MG, Brazil.
[f] Department of Plant Sciences, Forest Ecology and Conservation, University of Cambridge, Cambridge, UK.
[g] School of Forest Sciences, University of Eastern Finland. PO Box 111, Joensuu, Finland.
[h] Biosciences Laboratory, NASA Goddard Space Flight Center, Greenbelt, MD 20707, USA

ABSTRACT

Ambitious pledges to restore over 400 million hectares of degraded lands by 2030 have been made by several countries within the Global Partnership for Forest Landscape Restoration (FLR). Monitoring restoration outcomes at this scale requires cost-effective methods to quantify not only forest cover, but also forest structure and the diversity of useful species. Here we obtain and analyze structural attributes of forest canopies undergoing restoration in the Atlantic Forest of Brazil using a portable ground lidar remote sensing device as a proxy for airborne laser scanners. We assess the ability of these attributes to distinguish forest cover types, to estimate aboveground dry woody biomass (AGB) and to estimate tree species diversity (Shannon index and richness). A set of six canopy structure attributes were able to classify five cover types with an overall accuracy of 75%, increasing to 87% when combining two secondary forest classes. Canopy height and the unprecedented “leaf area height volume” (a cumulative product of canopy height and vegetation density) were good predictors of AGB. An index based on the height and evenness of the leaf area density profile was weakly related to the Shannon Index of tree species diversity and showed no relationship to species richness or to change in species composition. These findings illustrate the potential and limitations of lidar remote sensing for monitoring compliance of FLR goals of landscape multifunctionality, beyond a simple assessment of forest cover gain and loss.

KEYWORDS: Atlantic Forest; forest canopy; forest regeneration; forest succession; restoration accountability; restoration monitoring; tropical forest restoration; tropical reforestation.

INTRODUCTION

Current and future degradation have given rise to global (see Bonn Challenge, 2018) and regional (see WRI, 2018) pledges to restore vast areas of degraded and deforested landscapes, primarily in tropical areas and developing countries (Suding et al., 2015; Holl, 2017). These pledges have placed forests as integral components within a landscape management framework known as Forest Landscape Restoration (FLR). A product of an intergovernmental and interinstitutional dialogue, FLR goals will be accomplished by deliberately managing landscapes to generate a balance of social and ecological benefits (Sabogal et al., 2015). FLR strategies include natural regeneration, assisted natural regeneration, agroforestry, mixed species plantations and commercial monoculture plantations of different species (Laestadius et al., 2015; Aronson et al., 2017), that satisfy different stakeholders' preferences, ecological objectives and site requirements (Stanturf et al., 2014).

For such large-scale restoration initiatives, the increase in area covered by forest has been the primary indicator of outcome. Though forest cover can be a useful surrogate to evaluate primary productivity (Cao et al., 2016; del Castilho et al., 2018), it may be inadequate to represent other ecosystem functions, such as tree diversity, biogeochemical functions (Meli et al., 2017), or utility for livelihoods (Chazdon et al., 2016; Brancalion & Chazdon, 2017). Monitoring these more complex restoration outcomes requires additional procedures and tools. One logical procedure is, first, to distinguish the different forest cover types in the landscape (e.g., monoculture tree plantations, mixed second-growth forests and old-growth forests) and, second, to determine their respective values in terms of their contributions to biodiversity conservation and ecosystem services, such as carbon uptake and storage (Chazdon et al., 2016). Canopy structural attributes are useful for both distinguishing cover types and as indicators of their respective values. For instance, the aboveground dry wood biomass (AGB) is related to canopy height (Asner & Mascaro, 2014; Longo et al., 2016). Canopy openness has been used to assess tropical forest restoration success (Chaves et al., 2015; Viani et al., 2017). High tree species diversity, which benefits a greater range of stakeholders than monocultures do, may be related to the structural complexity of the vertical canopy profile (Isbell et al., 2011; Sapijanskas et al., 2014; Valbuena et al., 2016a).

A critical step for assessment of forest cover and function in the context of international FLR agreements is to develop replicable standard monitoring protocols that are cost efficient (Holl & Cairns, 2002). Traditional assessments of restoration outcomes rely heavily on field-based methods. Despite recent advances in participatory monitoring of FLR (Evans et al., 2018), these are cost-prohibitive and cannot track progress toward a commitment on the scale of millions of hectares (Holl, 2017). Over the past few years, novel remote sensing technologies such as lidar (light detection and ranging) have emerged as alternatives to monitoring forest structure, composition and function (Bergen et al., 2009; Stark et al., 2012; Hardiman, 2011; 2013. Simonson et al., 2014; Asner & Mascaro, 2014).

Lidar has the potential to penetrate the forest canopy (Lefsky et al., 2002). This give it the capacity to accurately measure structural canopy parameters such as forest height, canopy openness and leaf area density along the entire vertical profile (Stark et al., 2012; Almeida et al., 2016). This can be accomplished using either airborne or ground-based platforms. Some studies have used these lidar-derived attributes to distinguish forest types (Stark et al., 2012; Hardiman, 2011; 2013; Valbuena et al., 2013; 2016b), estimate AGB (Asner & Mascaro, 2014), and diversity of plant (Bergen et al., 2009) or animal species (Simonson et al., 2014). The efficacy of lidar for monitoring forest restoration is less known, particularly in tropical forests (Becknell et al., 2018; Mascaro et al., 2012).

Since airborne and ground lidar give similar values for structural metrics when applied to the same sites (Stark et al, 2012, 2015), a portable ground platform here is taken as an inexpensive proxy for extracting structure metrics that can also be retrieved from airborne laser scanning systems (ALS). The underlying justification of our study is to evaluate the feasibility of dispensing fully or partially with field inventories to monitor forest restoration outcomes (cover type, biomass and diversity) over very large areas using ALS.

Therefore, the objective of this study is to evaluate the potential of lidar technology to estimate key forest cover attributes in Brazil's Atlantic Forest region, an active forest restoration frontier. Using a portable ground platform, we quantitatively evaluate lidar’s potential to: (i) distinguish different forest cover types; (ii) estimate aboveground biomass; and (iii) estimate four metrics of tree species diversity and composition.

MATERIAL AND METHODS

Study sites and experimental design

We selected two locations having forest cover types commonly included in FLR programs (Table 1 and Figure 1). The first three cover types had natural spontaneous species compositions and the last three had planted tree species: (1) old-growth forests (“OG”); (2) second-growth forest established on former pastures (“SGpas”); or (3) on post-harvest *Eucalyptus* plantations with resprouting *Eucalyptus* trees dominating the canopy (“SGeuc”); (4) a set of planted restoration plots with differing tree species richness -- 20, 58 or 114 species (“PLdiv”); (5) another set of restoration plantations always having 20 tree species but with a managed range of aboveground biomass ("PLabg") (Campoe et al., 2014); and (6) mature eucalypt monoculture plantations ("Euc").

The three natural forest cover types – OG, SGpas and SGeuc – were seasonal semi-deciduous in the Atlantic Forest Biome of southeastern Brazil, in or near the Corumbataí River Basin (22°20' S, 47°40' W; 470-1060 m elevation). Site details are given in Cesar et al. (2018). The three planted cover types – PLdiv, PLagb, and Euc – were located at the Anhembi Forest Science Experiment Station of the University of São Paulo (22°43' S, 48°11' W, 455 m elevation and < 2% slope). See Ferez et al., (2015) for further Anhembi site description. Both the Corumbataí River basin and the Anhembi field station have a dry winter and a humid summer, mean annual precipitation of 1,100-1,367 mm and average temperature of 20-23°C (Köppen climate type Cwa) (Alvares et al., 2013).

We established 74 field sample plots in these six cover types (Table 1). We identified species and measured the diameter at breast height (DBH) for all individuals with DBH > 5 cm. Field work was in 2016-2017 and the time between field inventory and lidar measurements of forest structure was less than one year.

Table 1. Location (Corumbataí or Anhembi), forest cover type, sampling design (field plots and lidar data collection), and primary objectives of investigation (forest cover types, aboveground biomass, and tree diversity analysis).

Site	Forest cover types	Design	Objective: Tree cover type	Objective: Biomass	Objective: Diversity
Corumbataí	Old-growth Atlantic Coastal Forest ("OG").	4 plots of 900 m² (45x20 m), inventoried in 2016-2017. More than 100 years old. One 45-m Lidar transect in the plot center, collected in 2017.	Tree cover type	Biomass	Diversity
Corumbataí	Second-growth forests, spontaneous succession without human assistance on abandoned (post-harvest) Eucalpytus plantations ("SGeuc").	8 plots of 900 m² (45x20 m), inventoried in 2016-2017. Sucession ages (and number of plots) were 17 (1), 28 (1), 34 (3), and 45 (3) years. One 45-m Lidar transect in the plot center collected in 2017.	Tree cover type	Biomass	Diversity
Corumbataí	Second-growth forests, spontaneous succession without human assistance on abandoned cattle pastures of planted grasses ("SGpas").	11 plots of 900 m² (45x20 m), inventoried in 2016-2017. Sucession ages (and number of plots) were 11 (1), 20 (1), 30 (3), 34 (2) and 45 (4) years. One 45-m Lidar transect in the plot center collected in 2017.	Tree cover type	Biomass	Diversity
Anhembi	*Eucalyptus sp* plantation. ("Euc").	7 plots of 360 m² (45x8 m), inventoried in 2017. There were five plots of *E. urophylla* (three of 26 y and two of 37 y) and two plots of *E. grandis* (both 41 y old). One 45-m Lidar transect in the plot center collected in 2017.	Tree cover type		
Anhembi	Managed restoration plots with a specie richness gradient ("PLdiv").	12 plots of 2,160 m² (45x48 m), inventoried in 2016. There were four plots for each of three richness levels (20, 58 and 114 species), all 10 y old. Three parallel and equidistant 45-m Lidar transects in each plot, collected in 2016.	Tree cover type		Diversity
Anhembi	Managed restoration plots with a biomass gradient ("PLagb").	32 plots of 792 m² (36x22 m), inventoried in 2016. All plots had 20 planted tree species and were 13 y old. A factorial experiment of different types of management provided a biomass gradient (more details in Ferez et al., 2015). Two parallel and equidistant 45-m Lidar transects in each plot, collected in 2017.		Biomass	

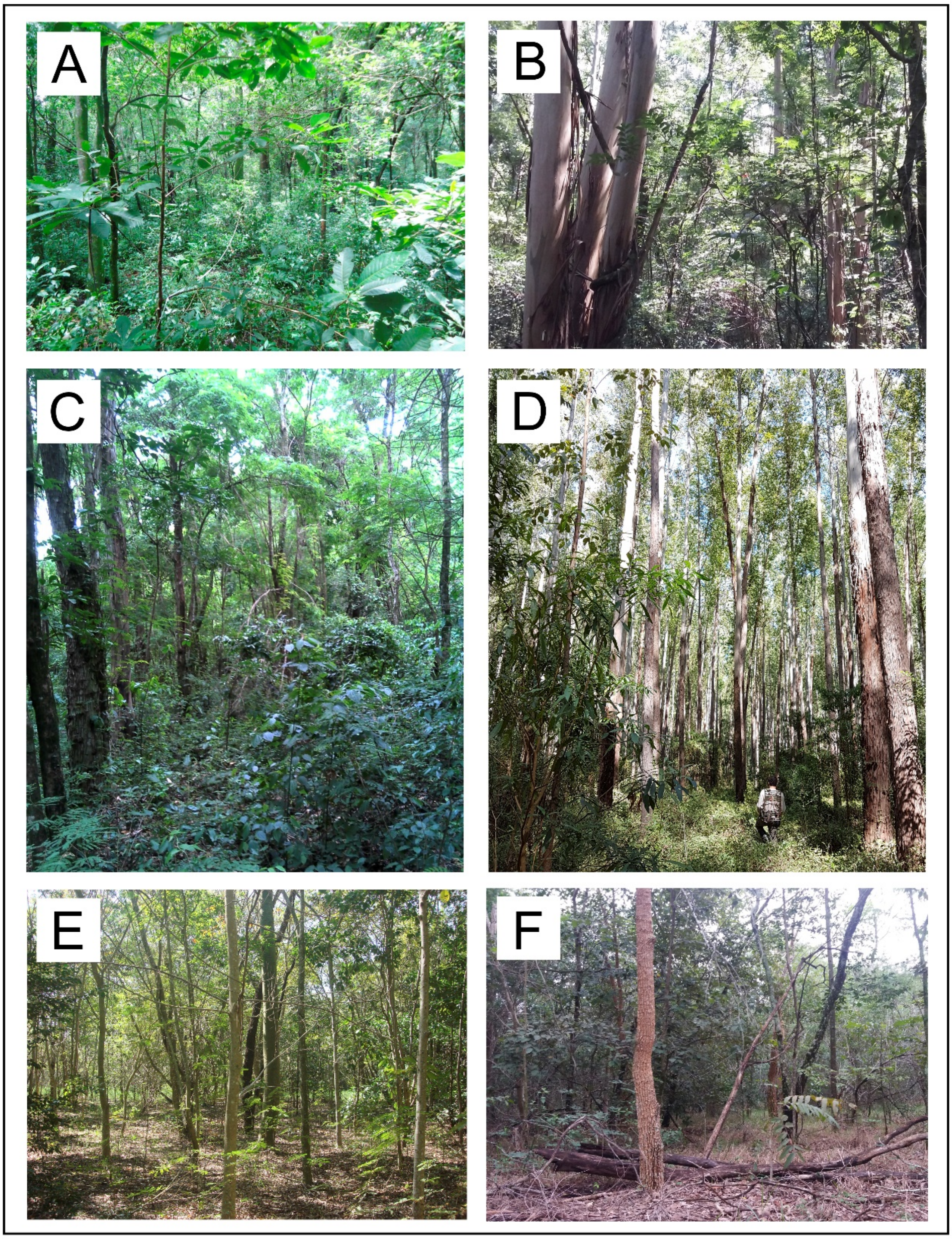

Figure 1. Forest cover types: (A) Old-growth Atlantic Coastal forest (OG); (B) Spontaneous second-growth forests that established after harvest of planted *Eucalyptus* spp. (SGeuc); (C) Spontaneous second-growth forests that established on grass-planted cattle pastures (SGpas); (D) monoculture *Eucalyptus* plantation (Euc); (E) Restoration areas planted with a species richness gradient across plots (PLdiv); and (F) Restoration areas planted with a biomass gradient across plots (PLagb).

Lidar-derived structural attributes

Ground-based lidar data were collected with the Portable Canopy profiling Lidar (PCL) system (Parker et al., 2004; Hardiman, 2011; 2013; Stark et al., 2012; Almeida et al., 2016), representing the capabilities of ALS. The PCL is a profiling range-finder type laser, model LD90-3100VHS-FLP manufactured by Riegl (Horn, Austria) that is carried by a walking operator along a transect. Surveys were conducted at a constant walking velocity (0.5 m/s), with a vertical upward view, producing a high-density 2D pulse return cloud (2,000 pulses per linear meter) along the transect.

Six continuous variables of forest canopy structure were estimated (all of which can also be extracted from ALS): (i) canopy height, as the average of the maximum heights from each 2-m along-track interval (Figure S1); (ii) canopy openness, as the fraction of 2-m along-track intervals with a maximum height less than 10 meters; (iii) canopy rugosity, as the standard deviation of maximum height at each 2-m interval; (iv) the mean leaf area index (LAI) of each transect; (v) the understory LAI, as the sum of the leaf area density (LAD) at all heights ≤ 5 m; and (vi) the leaf area height volume (LAHV, equation 1). For visual comparisons, and for extraction of some of the above variables, we also obtained a mean leaf area density (LAD, m^2 m^{-3}) profile of each transect.

LAD and LAI were estimated using the MacArthur-Horn equation (MacArthur & Horn, 1969) as described in Almeida et al. (2016). There is one mean LAD profile and one mean LAI value per plot transect. The former is a vertical stack of mean LADs, taking the mean of LAD horizontally at each 1-m height interval across all 2-m horizontal sections of transect. LAI is the sum of the mean LAD profile (Almeida et al., 2018).

LAHV, introduced in this study, is the sum of the products of height and mean LAD at that height, for all 1m height intervals in the mean LAD profile (Figure 2). There is one LAHV value per plot transect:

$$LAHV = \sum(i \times LAD_i) \quad (1)$$

where i (i = 1, 2, 3, …, max.height) is the height in the canopy and LAD_i is the horizontal mean of leaf area densities at the respective height (Figure 2). A geometrical interpretation of LAHV is that it sums the volumes bound by each unit of leaf area and the horizontal plane of the ground over all vertical positions. Biologically, leaf area and basal area are often assumed to be directly proportional, while cross sectional area of branches may be approximately constant over branching generations, and the number of branching generations increases linearly with height (West et al., 1997). Together this suggests that LAHV could be directly proportional to wood volume, and thus AGB (see model in Stark et al. 2015).

Total length of PCL transect per plot and field inventory plot sizes for each forest type are given in Table 1. Along each transect, the PCL beam has an oval footprint that samples about 4% and 11% of each 1 m deep (across-track) voxel at 5 m and 25 m height, respectively. The width of the forest inventory plot bisected by a PCL transect depends on crown size. For example, in *Eucalyptus* plantations crowns were small, so we used an 8-m-wide inventory plot. For the old-growth and secondary-growth forest canopies we used a 20-m wide plot. For the high diversity planted forest, we used two parallel PCL transects and a plot 48-m wide. Prior studies in Amazon forest have used PCL transects bisecting 20-m-wide plots and obtained satisfactory results (Almeida et al., 2016; Stark et al., 2012). Irrespective of plot size, the total PCL transect per plot should be long enough to provide a large number of sub-samples (columns of voxels) for a reliable estimate of mean LAD at each 1m height interval.

Data analysis

The inventory plots were the sampling units, and the lidar transects of these plots provided their structural attributes. For this reason, when multiple transects were made in a plot, we joined them into a single transect corresponding to that plot. For our first objective, to distinguish the forest cover types using only lidar-derived attributes, we used the Random Forests (RF) decision tree supervised classification. We included five of the six cover types listed in Table 1, excluding "PLagb" because it was considered not representative of typical restoration managed plots. Only when the purpose was forest cover type classification, we also added some lidar transects that were outside of the inventory plots to increase the number of observations per cover type, after ensuring that these transects belong to the same forest type. The sample size (number of plots and of transects) for OG, SGeuc, SGpas, PLdiv and Euc forest cover types were 18, 22, 35, 36 and 7, respectively.

We report the overall classification accuracy and the accuracies for each cover type in an error matrix. The error matrix was constructed from a jack-knife cross-validation. The optimal decision tree was obtained by including all but one randomly chosen transect in the training data, then seeing if the left-out transect was correctly classified. The RF classifier completed 10,000 iterations using all six continuous variables from lidar. We report the importance ranking of these six variables to overall classification accuracy and to the discrimination of each of the cover types. For a visual interpretation of the importance of each structural variable to the classifier we interpret critical features of the five LAD profiles. We also provide a two-dimensional depiction of the attribute hyperspace using principal components analysis (PCA). The PCA was based on the same six lidar-derived attributes of canopy structure that were used by the classifier, plus AGB from field inventories of the plots.

For our second objective – to examine the potential of lidar to estimate AGB – we used five cover types: three having spontaneously colonized tree plots (old-growth OG forest and two types of secondary growth, SGeu and SGpas), the *Eucalyptus* monoculture plots (Euc) and the biomass-managed planted tree plots (PLagb). In OG, SGeuc, and SGpas, the AGB of each plot was obtained from their DBH and wood density using the general allometric equation proposed by Chave et al. (2014). To estimate AGB of *Eucalyptus* spp. trees from their DBH, we used a specific equation developed locally by Campos et al. (1992). For the biomass-managed planted tree plots we used a multi-species allometric equation that uses DBH, wood density and tree height, developed from the mix of 20 tree species planted at the Anhembi experiment (Ferez et al. 2015). A multiple linear model was developed to estimate biomass from lidar attributes, after excluding attributes that did not satisfy assumptions of homoscedasticity, symmetric residuals or multi-collinearity. Simple linear regressions are also given for the best predictors of AGB. We computed the absolute and relative Root Mean Square Error (RMSE) for assessing the model accuracy (Eq. S1-S2).

For our third objective, to predict tree biodiversity from forest structure, diversity was represented in four different ways: species density (number of species per area using a fixed area); species richness for a fixed number of trees sampled from each plot by randomized rarefaction; tree community Shannon diversity index; and floristic composition. We considered floristic composition from the viewpoint of the score obtained on a single axis non-metric multidimensional scaling (NMDS). NMDS was in turn based on a triangular matrix containing all plot pairs' Jaccard similarity indices, using presence/absence of each species. All four diversity variables were obtained for the plots for the three cover types that had spontaneous natural colonization (OG, SGeuc, and SGpas). In the plots with 20, 58 or 114 planted tree species (cover type PLdiv) we used only species density, since the tree community Shannon index and the composition there were sensitive to the species density treatments. The single species monoculture (Euc) and the fixed 20-species biomass-managed plots (PLagb) were not included in the diversity prediction analyses.

The potential of lidar to provide a proxy for tree diversity was examined with an additional variable, the structure-based "canopy Shannon index" (Stark et al., 2012). The canopy Shannon Index is based on the mean LAD profile of a transect. It increases with the number of heights having vegetation present and with the equitability of LAD among those vegetated heights (McArthur & McArthur, 1961; Valbuena et al., 2012). We hypothesized that this index may be related to alpha species diversity at plot scale because the index would increase in older succession stages which are taller, having more vegetation strata, and because in OG forest dynamics allow specific tree species to colonize different canopy strata (Williams et al., 2017). Spearman correlations were obtained for the canopy Shannon index against each of the four tree biodiversity metrics (species density, species richness, tree community Shannon index, and floristic composition represented by NMDS score).

RESULTS

Lidar-derived structural attributes performed well as predictors of forest cover type and of the tree biomass of a plot, weakly as predictors of tree species evenness, and poorly as predictors of richness and difference in floristic composition between plots.

(i) *Discrimination of forest cover types using lidar*

Using six lidar-derived structure attributes, the Random Forests classifier identified the five forest cover types with an overall 75% accuracy (Table 2). The largest misidentifications were mutual between the two secondary forests; overall accuracy improved to 87% when these were combined as a single class. The importance of each structure variable to overall accuracy and to correct prediction of each forest cover type is shown in Table 3.

Table 2. Error matrix from a jack-knife validation of the Random Forests classifier of five forest cover types that used the six lidar-derived canopy structure variables shown in Table 3. Percent correct classification of each type is in bold on the diagonal; percent errors are off-diagonal. Types are: monoculture

Eucalyptus plantations (*Euc*), old-growth forests (*OG*), planted forests with three levels tree diversity combined here in a single class (PLdiv), spontaneous second-growth after harvest of a *Eucalyptus* plantation (*SGeuc*), and spontaneous second-growth on abandoned planted-grass cattle pastures (*SGpas*).

		True class				
		OG	*SGeuc*	*SGpas*	*PLdiv*	*Euc*
	OG	**77**	9	7		
	SGeuc	23	**51**	15		
Classified As:	*SGpas*		40	**61**	2	
	PLdiv			17	**98**	
	Euc					**100**

Overall accuracy = 75%

Lumping two secondary forests, overall accuracy = 87%

Table 3. Variable importance to classification accuracy. First column gives the mean decrease in overall percent accuracy of the classifier if just that variable is scrambled. Other cells, scaled 0-1 with red color ramp, indicate importance of each structural variable in classifying each forest cover type. Types are: monoculture *Eucalyptus* plantations (*Euc*), old-growth forests (*OG*), planted forests with three levels tree diversity combined here in a single class (PLdiv), spontaneous second-growth after harvest of a *Eucalyptus* plantation (*SGeuc*), and spontaneous second-growth on abandoned planted-grass cattle pastures (*SGpas*). LAI is the Leaf Area Index and LAHV is Leaf Area Height Volume.

		OG	SGeuc	SGpas	PLdiv	Euc
Canopy height	32.5	0.88	0.32	0.42	0.93	0.88
Canopy rugosity	31	0.13	0.94	0.35	0.96	0.34
Canopy openness	27	0.82	0.00	0.35	1.00	0.62
Understory LAI	23	0.31	0.05	0.42	0.79	0.77
LAI	20	0.36	0.26	0.36	0.51	0.63
LAHV	12	0.44	0.11	0.33	0.23	0.30

Forest cover types classified with highest accuracy had distinguishing features in their LAD profiles (Figure 2). Monoculture *Eucalyptus* plantations were classified with 100% accuracy and had the most distinctive profile: a tall canopy with low LAI and low canopy openness. The set of plots containing a range of diversity of planted trees (PLdiv) were identified with 95% accuracy. Compared with all the other forest cover types, these have a smoother canopy (single dominant height), low stature, and thus high fraction below 10m (high openness). The two second-growth forest types had very similar LAD profiles, and thus the RF classifier had difficulty in separating them.

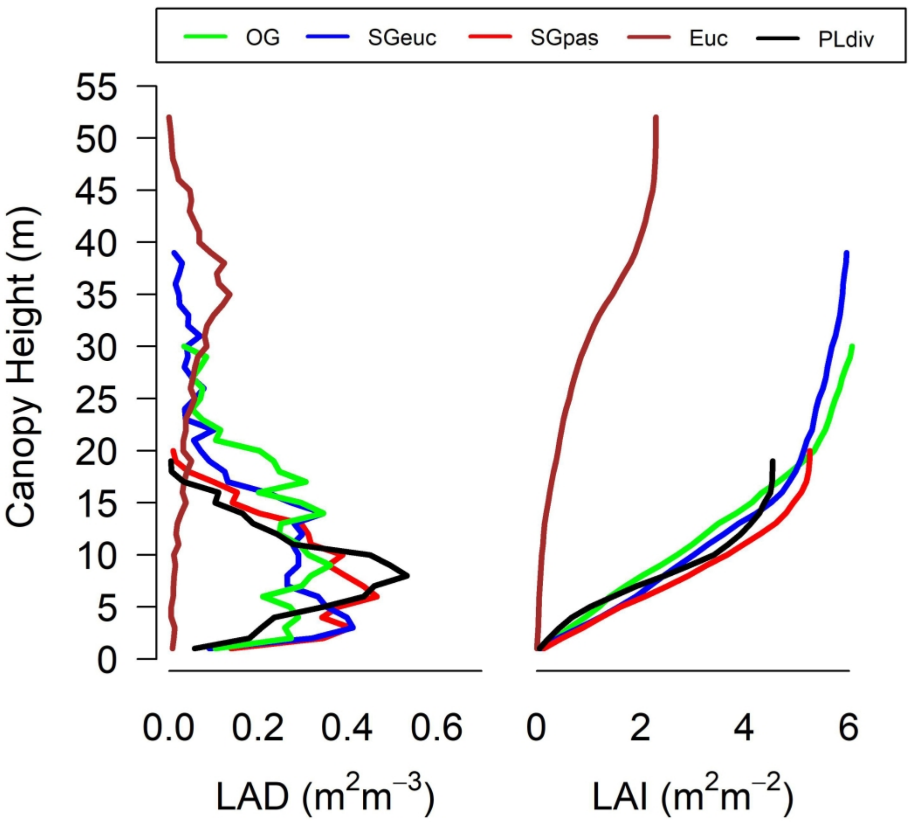

Figure 2. Mean leaf area density (LAD) profiles (left) and cumulative leaf area (LAI) (right) for the five forest cover types used in the classification accuracy assessment. Types are: monoculture *Eucalyptus* plantations (*Euc*), old-growth forests (*OG*), planted forests with three levels tree diversity combined here in a single class (PLdiv), spontaneous second-growth after harvest of a *Eucalyptus* plantation (*SGeuc*), and spontaneous second-growth on abandoned planted-grass cattle pastures (*SGpas*).

Further insights into how each lidar-derived structure variable contributes to the separation of cover classes by the classifier are evident in the scatterplot of scores for the first two PCA components (Figure 3), which explained 72% of total variance in the structural attribute hyperspace. The *Eucalyptus* plots, easily discriminated by the classifier, form a dense isolated cluster in the two-dimensional depiction. This is due to the odd combination of tall canopy but a low total LAI, with almost no understory (Table 3). Old-growth forest plots, classified with 88% accuracy, are pulled away from other cover types by their high aboveground biomass, tall canopy and low fraction of heights below 10m (low openness). Some of the plots of secondary forest developed on post-harvest *Eucalyptus*, are very rugose due to tall *Eucalyptus* stump sprouts; this attribute was useful to the best decision trees.

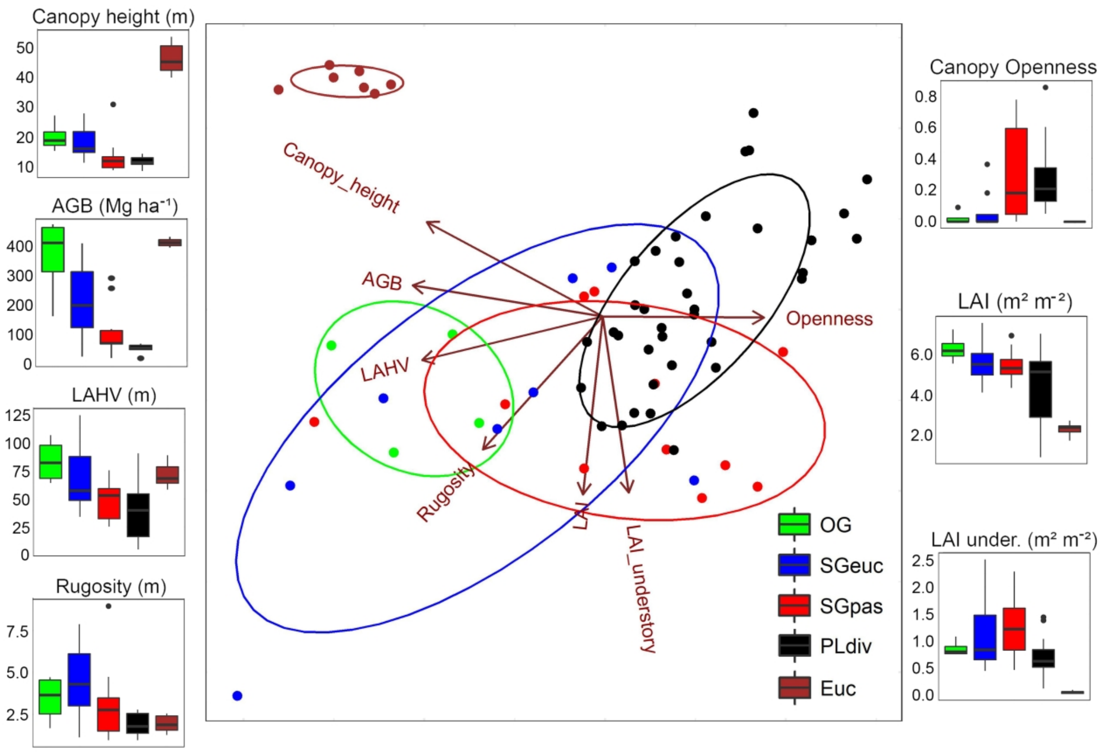

Figure 3. Biplot of the first two axes of a principal component analysis and boxplots of the seven canopy structural attributes used in the PCA (six lidar-derived plus the aboveground dry woody biomass). Forest cover types are coded by the same colors used in Fig. 2. Types are: monoculture *Eucalyptus* plantations (*Euc*), old-growth forests (*OG*), planted forests with three levels tree diversity combined here in a single class (PLdiv), spontaneous second-growth after harvest of a *Eucalyptus* plantation (*SGeuc*), and spontaneous second-growth on abandoned planted-grass cattle pastures (*SGpas*).

(ii) Predicting aboveground biomass from lidar

Across the three non-planted forest cover types, AGB was significantly correlated in simple regressions with three lidar-derived canopy structure attributes: LAHV, canopy height and LAI. Respective correlations with AGB were 0.84, 0.75, and 0.54 (Figure S2). Among the planted tree plots which have a biomass-managed gradient (PLagb), AGB was correlated with these same three structural attributes, with r = 0.75, 0.78, and 0.51, respectively (Figure S3). Canopy openness was discarded as it showed a strongly heteroscedastic, non-linear and saturated relationship with AGB.

While LHAV and canopy height each showed high explanatory value in simple regressions for the two sets of plots just described (Figure 4), they were highly correlated within each of these sets (r > 0.70). With all four forest cover types plus the *Eucalyptus* plantation in the same model, collinearity was reduced. Both predictors could be included in a multiple linear regression (Figure 5), obtaining $r^2 = 0.84$ (versus $r^2 = 0.69$ using only canopy height, $r^2 = 0.68$ using only LAHV; Figure S4).

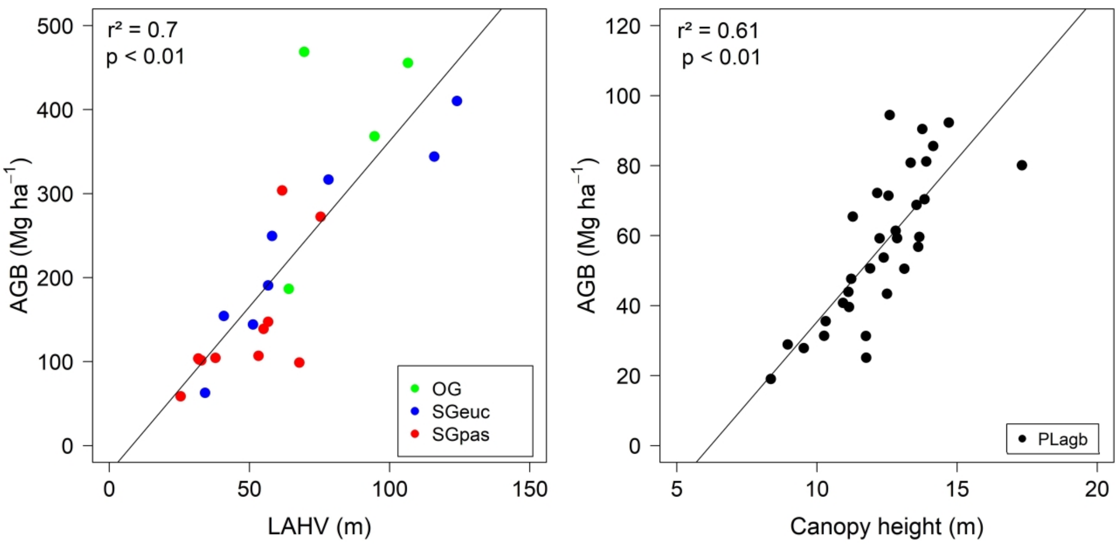

Figure 4. Aboveground biomass as a function of LAHV (left) for spontaneous vegetation (old-growth forests and two second-growth forests) ($r^2 = 0.7$, RMSE = 72.6, relative RMSE = 34.1%); and as a function of Canopy Height (right) for planted forest, (biomass-managed plots with 20 tree species) ($r^2 = 0.61$, RMSE = 13.5, relative RMSE = 23.8%).

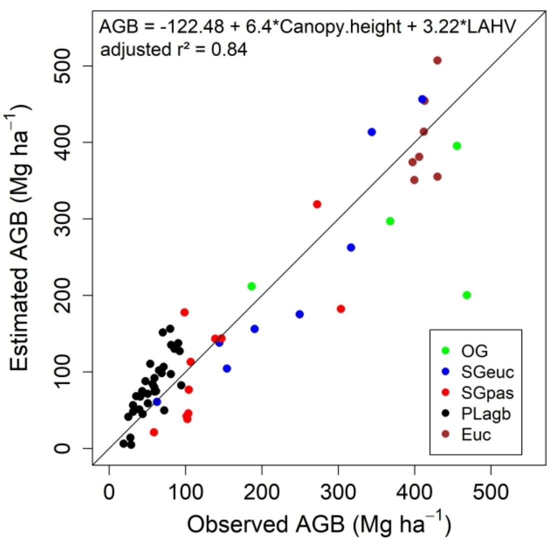

Figure 5. Multiple linear regression model using LAHV and Canopy Height as predictors of aboveground biomass (r^2 = 0.84, RMSE = 57, relative RMSE = 36,8%) of plots from five forest cover types: three spontaneous (old-growth plus two second growth types) and two planted (biomass-managed plots with 20 species and *Eucalyptus* monoculture).

(iii) Predicting tree diversity from lidar

About 25% of the variance in tree community Shannon diversity index could be explained using the purely structural "canopy Shannon index", when considering the set of plots in the three natural, spontaneously colonized forest cover types (Figure 6). The two indices were inversely related, which was unexpected. The other three measures of biological diversity -- species density, richness and composition NMDS score -- were not significantly related to canopy Shannon index (Figures S5 and S6).

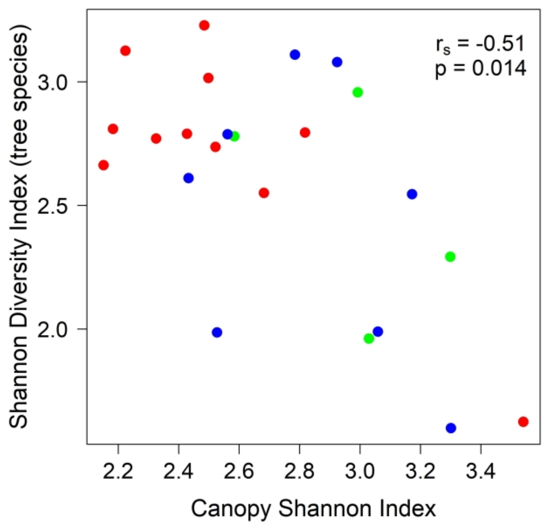

Figure 6. Scatterplot and Spearman's correlation between the canopy structure Shannon index derived from lidar and the floristic Shannon index for the set of three spontaneously colonized forest cover types: old-growth forests (green), secondary forest on former *Eucalyptus* plantation (blue), and second growth on former planted-grass pasture (red).

DISCUSSION

In this study, we characterized different restoration outcomes based on structural attributes derived from PCL, as a stand-in for airborne lidar capabilities. Those attributes were able to distinguish forest cover types and their associated AGB stocks and, to a lesser extent, tree species diversity. Previous studies have used Airborne Laser Scanner metrics to estimate AGB (Long et al., 2016) and to distinguish forest types (Stark et al., 2012; Gorgens et al., 2016) in patches and landscapes covered by old-growth native forests. However, few studies have analyzed forest restoration areas with discrete return lidar metrics (Becknell et al., 2018). The lack of studies analyzing the effectiveness of lidar technology for monitoring restoration is a critical limitation, as the structural and compositional heterogeneity of forest covers are expected to increase with different reforestation approaches, the existence of forest patches at different successional development stages, and the adoption of different management practices (Chazdon et al., 2016), and these approaches must be adequately compared.

Distinguishing different forest cover types

The attributes of canopy structure and of LAD profiles provided important indicators of structure and potential ecosystem functions of forest restoration components. The range of forest management and history was reflected in canopy structure. Second-growth forests originating from natural regeneration after 20-40 years showed attributes closer to old-growth forest. The restoration plantations, despite having high taxonomic diversity, are still an even-aged tree community with a more homogeneous canopy with vegetation density concentrated between about 5 and 12 m height. On the other hand, disturbances, succession, and longer time spans create a more heterogeneous canopy, as a consequence of the differential growth rates, turnover rates, and sensitivity to disturbances among tree species (Chazdon et al., 2014).

In the old-growth forests, LAD was better distributed throughout the vertical canopy profile, impacting tree growth and survival and generating a diversity of niches for birds, insects, epiphylls and microbes that are host-specific or that occupy different heights of the canopy (McDonnell, 1986; Zahawi et al., 2015), all factors with potential impacts on canopy ecosystem functions. The spread of vegetation along the vertical profile can also be observed in cumulative LAI curves, where the old-growth forests had a higher LAI and a more constant increase in LAI compared to the other forest cover types. SGeuc presented a structure similar to old-growth forest. Second-growth from pasture (SGpas) may take longer to reach such tall canopy structure with shaded understory. Some studies have found no negative effect of *Eucalyptus* spp. on growth of juvenile native tree species in the Atlantic Forest region (Cesar et al., 2018; Amazonas et al., 2018). The structure of intensively managed, monoculture eucalypt plantations was, however, markedly different from the other forest cover types, lacking vegetation at low or medium vertical strata, suggesting inhibition by shade and/or the novel weapons (allelopathic biochemicals) produced by this non-native genus (Becerra et al., 2017). Although eucalypt plantations had a taller canopy, the LAHV (leaf area height volume) was higher in old-growth.

Aboveground biomass estimation from lidar

Other studies have demonstrated the potential of canopy-structure metrics derived from airborne scanning lidar point clouds for estimating forest biomass (Longo et al., 2016; Mascaro & Asner, 2015). LAHV, a novel canopy structure metric presented for the first time in this study, shows promise as an additional variable for general biomass equations, since it includes both height and LAD information. Height alone is not a consistent predictor of biomass. In our study, old- and second-growth forests (>100 and 20-40 years old, respectively) had height x biomass relationships than were different from those in the restoration plantation/biomass experiment (13 years old) (see Figure 4). LAHV also was useful for qualifying forest cover and assessing its diverse functions.

Other variables also showed significant relationships with AGB. For airborne lidar data, canopy openness is an important metric for estimating AGB and assessing canopy dynamics (Mascaro & Asner, 2015; Leitold et al., 2018). Airborne lidar has the potential to measure the canopy structure continuously, on a fine scale and over large areas. This provides spatial context allowing classification of plot forest cover type using object based image analysis, not possible with PCL transects.

Our results highlight the need to consider different models to estimate AGB in the context of FLR, particularly for the species-rich, structurally complex forests found in tropical regions. We chose to use site and taxa specific AGB allometries in this study because universal relationships (e.g., Chave et al., 2014) may have lower accuracy. Likewise, the relationship between AGB and canopy structural characteristics is a function of the specific architectures and allometries that relate leaf area and its vertical positions to basal area, wood volume, and wood density biomass (Stark et al., 2015). Species and taxonomic differences cannot be completely factored out to produce accurate AGB estimates from lidar, and field inventory approaches can never completely fulfill the needs of forest restoration monitoring alone. Taxonomic and functional information, particularly wood density, improves AGB estimates. These factors may have contributed to our finding that AGB of different forest cover types were best predicted by different structural attributes and equations. Nonetheless a simple linear model with two predictors, canopy height and LAHV, explained over 80% of the variation in estimated biomass of plots from different cover types, suggesting that a parsimonious set of architectural rules govern forest biomass.

Tree community diversity estimation from Lidar

Estimation of tree diversity is one of the challenges of remote sensing (Turner et al., 2003; Bergen et al., 2009; Simonson et al., 2015). Some studies have linked tree diversity with vegetation structure in temperate forests (Bergen et al., 2009) and the combination of lidar and hyperspectral data has shown promising results towards this objective (Asner et al., 2015). For the three non-planted forest types, we found a weak inverse relationship between the canopy structure Shannon index (SI) and the tree species diversity SI. Species richness by itself was not related to canopy structure SI. These are unexpected patterns, since mature and late succession forests should be species-rich with no dominant species (high tree diversity SI) and should also be taller with more canopy strata occupied by vegetation (high structure SI). A possible explanation is the lack of early succession plots in our mix, as these would be of short height (low structure SI) and would have few species, some of which dominant (low tree diversity SI). Additional work is required, encompassing a broader range of diversity and succession ages to validate this relationship, explore evenness and richness independently, and investigate potential mechanistic relationships driving the interaction between tree diversity and canopy structure (Sapijanskas et al., 2014; Williams et al., 2017).

Monitoring forest restoration outcomes with lidar

Qualitative and quantitative indicators of forest recovery are needed to support policies that successfully protect, sustain, and recover forests at multiple scales and for different objectives (Chazdon et al., 2016). Though we found a limited potential for lidar to estimate tree diversity or composition, it clearly distinguished different patterns of carbon recovery. This is noteworthy given the growing global interest in FLR and the service that restored forests provide to mitigate climate change (Grassi et al., 2017; Griscom et al., 2017). Current FLR restoration goals are ambitious and require cost-efficient solutions. Lidar will clearly be part of a suite of protocols that must be developed for monitoring restoration frequently at large spatial scales and at low cost. Here we have provided insights on the further adoption and application of PCL as an accessible and powerful complementary data stream to improve understanding of the consequences of restoration for carbon stocks and forest services, which could be further developed with airborne lidar (Stark et al., 2012). All the canopy structural attributes derived from PCL used in this study can also be estimated using an airborne system (Stark et al., 2012; Almeida et al., *2019*). Thus, portable terrestrial lidar monitoring serves as an inexpensive proxy for airborne lidar. But only the latter can ultimately provide data on forest structure rapidly and over broad geographic scopes. Lidar brings additional insights to monitoring recovery of forest functionality at large-scales in the future. Stark et al. (2015) used vegetation density profiles to estimate the demographic distribution of trees, which is key to inferring forest successional stage. Airborne lidar also enables the preparation of digital terrain models with high accuracy (Leitold et al., 2015), useful for the planning of restoration projects (Schulz et al. 2016).

The relationship between lidar metrics and forest structure and composition can be affected by plot size. Larger plots have the potential to reduce the uncertainty in the estimation of structure attributes (Asner and Mascaro, 2014). In this study we tried to standardize plot size at 800-900 m^2. The Shannon Index of species diversity adjusts for sample size. Nonetheless, larger samples are recommended for more diverse communities, while smaller samples are sufficient for monocultures. So, we reduced plot size to 360 m^2 in the Eucalyptus plantations and increased to 2160 m^2 in the set of restoration plots having a planted tree species diversity gradient.

Our study provides insights into monitoring forest restoration outcomes beyond simple forest cover extent and cover gain, in a more integrated approach that includes indicators of diversity and of ecosystem function. Though we evaluated these outcomes at a local scale, our results contribute to the discussion at landscape scale regarding the need of FLR to include the full heterogeneous mosaic of expected forest cover types. For example, assessing potential relationships between different forest structure, forest types and tree community beta diversity at landscape scales may prove challenging, but nevertheless is a promising avenue. Effective monitoring of FLR programs is important not only for accountability and tracking progress towards national, regional, and international restoration commitments. It is also a key step to improve current restoration approaches and to develop novel methods that are better suited for the different socio-ecological conditions under which FLR will be implemented.

CONCLUSION

Lidar-derived structural variables performed well for discriminating forest cover types. Canopy height, rugosity and openness were the most useful attributes. Leaf area height volume (LAHV) was of low value for classification but improved estimation of biomass. The structural attribute “canopy Shannon Index”, which was tested as the single predictor of tree diversity and composition, proved to be of limited value for this purpose. Combining classification outputs with the canopy Shannon Index would, however, improve biodiversity estimation as the low diversity monoculture was identified with 100% accuracy. We have shown lidar to be a promising tool for monitoring multiple of forest restoration project objective outcomes, beyond a simple binary classification of forest cover. Further evaluation is recommended as the next step, including a broader range of cover types and ages.

ACKNOWLEDGEMENTS

Funding was provided by São Paulo Research Foundation (FAPESP) grants #2016/05219-9 and #2014/14503-7 and CAPES. P. Meli was supported by FAPESP grant

#2016/00052-9, R. Valbuena by the EU Horizon2020 Marie Sklodowska-Curie Action LORENZLIDAR (658180), and S. C. Stark by NSF (EF-1550686 and EF-1340604). We thank João Carlos Teixeira Mendes, coordinator of Anhembi Research Station (ESALQ - USP), for his contributions to field work.

REFERENCES

Abshire, J. B., Sun, X., Riris, H., Sirota, J. M., McGarry, J. F., Palm, S., … Liiva, P. (2005). Geoscience Laser Altimeter System (GLAS) on the ICESat mission: On-orbit measurement performance. *Geophysical Research Letters*, *32*(21), 1–4. doi:10.1029/2005GL024028

AICHI TARGETS. Link: https://www.cbd.int/sp/targets/. Acceded em 21/05/2018.

Alexander, S., Nelson, C. R., Aronson, J., Lamb, D., Cliquet, A., Erwin, K. L., … Murcia, C. (2011). Opportunities and Challenges for Ecological Restoration within REDD+. *Restoration Ecology*. doi:10.1111/j.1526-100X.2011.00822.x

Almeida, D. R. A. de, Nelson, B. W., Schietti, J., Gorgens, E. B., Resende, A. F., Stark, S. C., & Valbuena, R. (2016). Contrasting fire damage and fire susceptibility between seasonally flooded forest and upland forest in the Central Amazon using portable profiling LiDAR. *Remote Sensing of Environment*, *184*, 153–160. doi:10.1016/j.rse.2016.06.017

Almeida, D. R. A.; Stark, S. C.; Shao, G.; Schietti, J.; Nelson, B. W.; Silva, C. A.; Gorgens, E. B.; Valbuena, R; Papa, D. A.; Brancalion, P. H. S. (2019). Optimizing the remote detection of tropical rainforest structure with airborne lidar: leaf area profile sensitivity to pulse density and spatial sampling. *Remote Sensing*. doi:10.3390/rs11010092

Alvares, C. A., Stape, J. L., Sentelhas, P. C., De Moraes Gonçalves, J. L., & Sparovek, G. (2013). Köppen's climate classification map for Brazil. *Meteorologische Zeitschrift*. doi:10.1127/0941-2948/2013/0507

Amazonas, N. T., Forrester, D. I., Silva, C. C., Almeida, D. R. A., Rodrigues, R. R., & Brancalion, P. H. S. (2018). High diversity mixed plantations of *Eucalyptus* and native trees: An interface between production and restoration for the tropics. *Forest Ecology and Management*, *417*, 247–256. doi:10.1016/j.foreco.2018.03.015

Aronson, J., Blignaut, J. N., & Aronson, T. B. (2017). Conceptual Frameworks and References for Landscape-scale Restoration: Reflecting Back and Looking Forward. *Annals of the Missouri Botanical Garden*, *102*(2), 188–200. doi:10.3417/2017003

Asner, G. P., Mascaro, J., Muller-Landau, H. C., Vieilledent, G., Vaudry, R., Rasamoelina, M., ... & Van Breugel, M. (2012). A universal airborne LiDAR approach for tropical forest carbon mapping. Oecologia, 168(4), 1147-1160. doi: 10.1007/s00442-011-2165-z

Asner, G. P., & Mascaro, J. (2014). Mapping tropical forest carbon: Calibrating plot estimates to a simple LiDAR metric. *Remote Sensing of Environment*, *140*, 614–624. doi:10.1016/j.rse.2013.09.023

Asner, G. P., Ustin, S. L., Townsend, P. A., Martin, R. E., & Chadwick, K. D. (2015). Forest biophysical and biochemical properties from hyperspectral and LiDAR remote sensing. *Land Resources Monitoring, Modeling and Mapping with Remote Sensing. CRC Press, Taylor & Francis Group*, 429–448.

Becerra, P. I., Catford, J. A., Luce McLeod, M., Andonian, K., Aschehoug, E. T., Montesinos, D., & Callaway, R. M. (2018). Inhibitory effects of Eucalyptus globulus on understorey plant growth and species richness are greater in non-native regions. *Global Ecology and Biogeography*. doi:10.1111/geb.12676

Becknell, J. M., Keller, M., Piotto, D., Longo, M., Nara dos-Santos, M., Scaranello, M. A., … Porder, S. (2018). Landscape-scale lidar analysis of aboveground biomass distribution in secondary Brazilian Atlantic Forest. *Biotropica*. doi:10.1111/btp.12538

Bergen, K. M., Goetz, S. J., Dubayah, R. O., Henebry, G. M., Hunsaker, C. T., Imhoff, M. L., … Radeloff, V. C. (2009). Remote sensing of vegetation 3-D structure for biodiversity and habitat: Review and implications for lidar and radar spaceborne missions. *Journal of Geophysical Research: Biogeosciences*. doi:10.1029/2008JG000883

BONN CHALLENGE. Link: http://www.bonnchallenge.org/. Acceded in 21/05/2018

Bonner, M. T. L., Schmidt, S., & Shoo, L. P. (2013). A meta-analytical global comparison of aboveground biomass accumulation between tropical secondary forests and monoculture plantations. *Forest Ecology and Management*, *291*, 73–86. doi:10.1016/j.foreco.2012.11.024

Brancalion, P. H. S., & Chazdon, R. L. (2017). Beyond hectares: four principles to guide reforestation in the context of tropical forest and landscape restoration. *Restoration Ecology*. doi:10.1111/rec.12519

Brancalion, P. H. S., Schweizer, D., Gaudare, U., Mangueira, J. R., Lamonato, F., Farah, F. T., … Rodrigues, R. R. (2016). Balancing economic costs and ecological outcomes of passive and active restoration in agricultural landscapes: the case of Brazil. *Biotropica*, *48*(6), 856–867. doi:10.1111/btp.12383

Brancalion, P. H. S., Viani, R. A. G., Calmon, M., Carrascosa, H., & Rodrigues, R. R. (2013). How to Organize a Large-Scale Ecological Restoration Program? The Framework Developed by the Atlantic Forest Restoration Pact in Brazil. *Journal of Sustainable Forestry*, *32*(7), 728–744. doi:10.1080/10549811.2013.817339

Campoe, O. C., Iannelli, C., Stape, J. L., Cook, R. L., Mendes, J. C. T., & Vivian, R. (2014). Atlantic forest tree species responses to silvicultural practices in a degraded pasture restoration plantation: From leaf physiology to survival and initial growth. *Forest Ecology and Management*. doi:10.1016/j.foreco.2013.11.016

Campos, J. C. C., J. A. Silva, and B. R. Vital. 1992. Volume e biomassa do tronco e da copa de eucalipto de grande porte. Revista Árvore 16:319–336.

Cao, S., Sanchez-Azofeifa, G. A., Duran, S. M., & Calvo-Rodriguez, S. (2016). Estimation of aboveground net primary productivity in secondary tropical dry forests using the Carnegie-Ames-Stanford approach (CASA) model. *Environmental Research Letters*, *11*(7). doi:10.1088/1748-9326/11/7/075004

César, R. G., Moreno, V. S., Coletta, G. D., Chazdon, R. L., Ferraz, S. F. B., De Almeida, D. R. A., & Brancalion, P. H. S. (2018). Early ecological outcomes of natural regeneration and tree plantations for restoring agricultural landscapes. *Ecological Applications*, *28*(2). doi:10.1002/eap.1653

Chave, J., Réjou-Méchain, M., Búrquez, A., Chidumayo, E., Colgan, M. S., Delitti, W. B. C., … Vieilledent, G. (2014). Improved allometric models to estimate the aboveground biomass of tropical trees. *Global Change Biology*, *20*(10), 3177–3190. doi:10.1111/gcb.12629

Chaves, R. B., Durigan, G., Brancalion, P. H. S., & Aronson, J. (2015). On the need of legal frameworks for assessing restoration projects success: new perspectives from São Paulo state (Brazil). *Restoration Ecology*. doi:10.1111/rec.12267

Chazdon, R. L. (2014). Second Growth: The Promise of Tropical Forest Regeneration in an Age of Deforestation. Journal of Chemical Information and Modeling. doi:10.1017/CBO9781107415324.004

Chazdon, R. L., Brancalion, P. H. S., Laestadius, L., Bennett-Curry, A., Buckingham, K., Kumar, C., … Wilson, S. J. (2016). When is a forest a forest? Forest concepts and definitions in the era of forest and landscape restoration. *Ambio*, *45*(5), 538–550. doi:10.1007/s13280-016-0772-y

Chazdon, R. L., Brancalion, P. H. S., Lamb, D., Laestadius, L., Calmon, M., & Kumar, C. (2017). A Policy-Driven Knowledge Agenda for Global Forest and Landscape Restoration. *Conservation Letters*, *10*(1), 125–132. doi:10.1111/conl.12220

del Castillo, E. G., Sanchez-Azofeifa, A., Gamon, J. A., Avendaño, M. Q., & others. (2018). Integrating proximal broad-band vegetation indices and carbon fluxes to model gross primary productivity in a tropical dry forest. Environmental Research Letters. doi: 10.1088/1748-9326/aac3f0

Don, A., Schumacher, J., & Freibauer, A. (2011). Impact of tropical land-use change on soil organic carbon stocks - a meta-analysis. *Global Change Biology*. doi:10.1111/j.1365-2486.2010.02336.x

Evans, K., Guariguata, M. R., & Brancalion, P. H. S. (2018). Participatory monitoring to connect local and global priorities for forest restoration. *Conservation Biology*. doi:10.1111/cobi.13110

Ferez, A. P. C., Campoe, O. C., Mendes, J. C. T., & Stape, J. L. (2015). Silvicultural opportunities for increasing carbon stock in restoration of Atlantic forests in Brazil. Forest Ecology and Management, 350, 40-45. doi: 10.1016/j.foreco.2015.04.015

FLR. Link: http://www.forestlandscaperestoration.org/. Acceded in 21/05/2018

Grassi, G., House, J., Dentener, F., Federici, S., Den Elzen, M., & Penman, J. (2017). The key role of forests in meeting climate targets requires science for credible mitigation. *Nature Climate Change*. doi:10.1038/nclimate3227

Griscom, B. W., Adams, J., Ellis, P. W., Houghton, R. A., Lomax, G., Miteva, D. A., … Fargione, J. (2017). Natural climate solutions. *Proceedings of the National Academy of Sciences*. doi:10.1073/pnas.1710465114

GEDI. https://science.nasa.gov/missions/gedi. Acceded in 05/25/2018.

Görgens, E. B., Soares, C. P. B., Nunes, M. H., & Rodriguez, L. C. E. (2016). Characterization of Brazilian forest types utilizing canopy height profiles derived from airborne laser scanning. *Applied Vegetation Science*, *19*(3), 518–527. doi:10.1111/avsc.12224

Hardiman, B. S., Bohrer, G., Gough, C. M., Vogel, C. S., & Curtis, P. S. (2011). The role of canopy structural complexity in wood net primary production of a maturing northern deciduous forest. *Ecology*, *92*(9), 1818–1827. doi:10.1890/10-2192.1

Hardiman, B. S., Gough, C. M., Halperin, A., Hofmeister, K. L., Nave, L. E., Bohrer, G., & Curtis, P. S. (2013). Maintaining high rates of carbon storage in old forests: A mechanism linking canopy structure to forest function. *Forest Ecology and Management*. doi:10.1016/j.foreco.2013.02.031

Helmer, E. H., Lefsky, M. A., & Roberts, D. A. (2009). Biomass accumulation rates of Amazonian secondary forest and biomass of old-growth forests from Landsat time series and the Geoscience Laser Altimeter System. *Journal of Applied Remote Sensing*, *3*(1), 33505. doi:https://doi.org/10.1117/1.3082116

Holl, K. D., & Cairns, J. (2002). Monitoring and appraisal. In: M. R. Perrow, & A. J. Davy (Eds.). Handbook of ecological restoration (pp. 411–432). Cambridge, England: Cambridge University Press.

Holl, K. D. (2017). Restoring tropical forests from the bottom up. *Science*. doi:10.1126/science.aam5432

IBEMA. https://www.funcate.org.br/msa/projetos/mudanca-de-uso-da-terra. Acceded in 05/25/2018.

Laestadius, L., Buckingham, K., Maginnis, S., & Saint-Laurent, C. (2015). Back to Bonn and beyond: A history of forest landscape restoration and an outlook for the future. *Unasylva*, *245*, 11–18.

Lefsky, M. A., Cohen, W. B., Parker, G. G., & Harding, D. J. (2002). Lidar remote sensing for ecosystem studies. *BioScience*, *52*(1), 19–30. doi:10.1641/0006-3568(2002)052[0019:LRSFES]2.0.CO;2

Leitold, V., Michael Keller, Douglas C Morton, Bruce D Cook, & Yosio E Shimabukuro. (2014). Airborne lidar-based estimates of tropical forest structure in complex terrain: Opportunities and trade-offs for REDD+. Carbon Balance and Management, 10(1). doi:10.1186/s13021-015-0013-x

Longo, M., Keller, M., dos-Santos, M. N., Leitold, V., Pinagé, E. R., Baccini, A., … Morton, D. C. (2016). Aboveground biomass variability across intact and degraded forests in the Brazilian Amazon. *Global Biogeochemical Cycles*, *30*(11), 1639–1660. doi:10.1002/2016GB005465

McArthur, R.H. & McArthur, J.W. (1961). On bird species diversity. *Ecology* 42, 594–598.

McDonnell, M. J. (1986). Old field Vegetation Height and the Dispersal Pattern of Bird-Disseminated Woody Plants. *Bulletin of the Torrey Botanical Club*, *113*(1), 6. doi:10.2307/2996227

Mascaro, J., Asner, G. P., Dent, D. H., DeWalt, S. J., & Denslow, J. S. (2012). Scale-dependence of aboveground carbon accumulation in secondary forests of Panama: A test of the intermediate peak hypothesis. *Forest Ecology and Management*, *276*, 62–70. doi:10.1016/j.foreco.2012.03.032

Meli, P., Holl, K. D., Benayas, J. M. R., Jones, H. P., Jones, P. C., Montoya, D., & Mateos, D. M. (2017). A global review of past land use, climate, and active vs. passive restoration effects on forest recovery. *PLoS ONE*.

doi:10.1371/journal.pone.0171368

Menz, M. H. M., Dixon, K. W., & Hobbs, R. J. (2013). Hurdles and opportunities for landscape-scale restoration. *Science*. doi:10.1126/science.1228334

Pistorius, T., & Freiberg, H. (2014). From target to implementation: Perspectives for the international governance of forest landscape restoration. *Forests*, *5*(3), 482–497. doi:10.3390/f5030482

Saatchi, S. S., Harris, N. L., Brown, S., Lefsky, M., Mitchard, E. T. A., Salas, W., … Morel, A. (2011). Benchmark map of forest carbon stocks in tropical regions across three continents. *Proceedings of the National Academy of Sciences*, *108*(24), 9899–9904. doi:10.1073/pnas.1019576108

Sabogal, C., Besacier, C., & McGuire, D. (2015). Forest and landscape restoration: concepts, approaches and challenges for implementation. *Unasylva*, *66*(245), 3.

Sapijanskas, J., Paquette, A., Potvin, C., Kunert, N., & Loreau, M. (2014). Tropical tree diversity enhances light capture through crown plasticity and spatial and temporal niche differences. *Ecology*. doi:10.1890/13-1366.1

Schulz, J. J., & Schröder, B. (2017). Identifying suitable multifunctional restoration areas for Forest Landscape Restoration in Central Chile. Ecosphere, 8(1). doi: 10.1002/ecs2.1644

Silva, C. A., Hudak, A. T., Vierling, L. A., Klauberg, C., Garcia, M., Ferraz, A., … Saatchi, S. (2017). Impacts of airborne lidar pulse density on estimating biomass stocks and changes in a selectively logged tropical forest. *Remote Sensing*, *9*(10). doi:10.3390/rs9101068

Simonson, W. D., Allen, H. D., & Coomes, D. A. (2014). Applications of airborne lidar for the assessment of animal species diversity. *Methods in Ecology and Evolution*. doi:10.1111/2041-210X.12219

Souza Jr, C. M., Siqueira, J. V., Sales, M. H., Fonseca, A. V., Ribeiro, J. G., Numata, I., ... & Barlow, J. (2013). Ten-year Landsat classification of deforestation and forest degradation in the Brazilian Amazon. Remote Sensing, 5(11), 5493-5513. doi:10.3390/rs5115493

Stanturf, J. A., Palik, B. J., & Dumroese, R. K. (2014). Contemporary forest restoration: A review emphasizing function. *Forest Ecology and Management*. doi:10.1016/j.foreco.2014.07.029

Suding, K., Higgs, E., Palmer, M., Callicott, J. B., Anderson, C. B., Baker, M., … Schwartz, K. Z. S. (2015). Committing to ecological restoration. *Science*, *348*(6235), 638–640. doi:10.1126/science.aaa4216

Tang, H., Dubayah, R., Swatantran, A., Hofton, M., Sheldon, S., Clark, D. B., & Blair, B. (2012). Retrieval of vertical LAI profiles over tropical rain forests using waveform lidar at la selva, costa rica. *Remote Sensing of Environment*, *124*, 242–250. doi:10.1016/j.rse.2012.05.005

Tilley, B. K., Munn, I. A., Evans, D. L., Parker, R. C., & Roberts, S. D. (2005). Cost considerations of using LiDAR for timber inventory. *The 2004 Annual Southern Forest Economics Workshop.*, 43–50. Retrieved from http://sofew.cfr.msstate.edu/papers/0504tilley.pdf

Turner, W., Spector, S., Gardiner, N., Fladeland, M., Sterling, E., & Steininger, M. (2003). Remote sensing for biodiversity science and conservation. *Trends in Ecology and Evolution*. doi:10.1016/S0169-5347(03)00070-3

Valbuena, R., Packalén, P., Martín-Fernández, S., & Maltamo, M. (2012). Diversity and equitability ordering profiles applied to study forest structure. *Forest Ecology and Management* 276(0): 185–195. doi:10.1016/j.foreco.2012.03.036.

Valbuena R., Packalen P., García-Abril A., Mehtätalo L. & Maltamo M. (2013) Characterizing Forest Structural Types and Shelterwood Dynamics from Lorenz-based Indicators Predicted by Airborne Laser Scanning. *Canadian Journal of Forest Research* 43: 1063-1074. doi: 10.1139/cjfr-2013-0147

Valbuena R., Maltamo M. & Packalen P. (2016a) Classification of Multi-Layered Forest Development Classes from Low-Density National Airborne Lidar Datasets. *Forestry* 89: 392-341. doi: 10.1093/forestry/cpw010

Valbuena R., Eerikäinen K., Packalen P. & Maltamo M. (2016b) Gini Coefficient Predictions from Airborne Lidar Remote Sensing Display the Effect of Management Intensity on Forest Structure. *Ecological Indicators* 60: 574-585. doi: 10.1016/j.ecolind.2015.08.001

Viani, R. A., Holl, K. D., Padovezi, A., Strassburg, B. B., Farah, F. T., Garcia, L. C., ... & Brancalion, P. H. (2017). Protocol for monitoring tropical forest restoration: perspectives from the Atlantic forest restoration pact in Brazil. Tropical *Conservation Science*, 10. doi: 10.1177/1940082917697265.

West, G. B., Brown, J. H., & Enquist, B. J. (1997). A general model for the origin of allometric scaling laws in biology. *Science*. doi:10.1126/science.276.5309.122

Williams, L. J., Paquette, A., Cavender-Bares, J., Messier, C., & Reich, P. B. (2017). Spatial complementarity in tree crowns explains overyielding in species mixtures. *Nature Ecology and Evolution*. doi:10.1038/s41559-016-0063

WRI, 2018. Initiative 20x20. World Resources Institute. http://www.wri.org/our-work/project/initiative-20x20/about-initiative-20x20#project-tabs. Acceded in 05/28/2018.

Zahawi, R. A., Dandois, J. P., Holl, K. D., Nadwodny, D., Reid, J. L., & Ellis, E. C. (2015). Using lightweight unmanned aerial vehicles to monitor tropical forest recovery. *Biological Conservation*, *186*, 287–295. doi:10.1016/j.biocon.2015.03.031

The effectiveness of Lidar remote sensing for monitoring tree cover attributes in forest and landscape restoration

Almeida, D. R. A.[a]; Stark, S. C.[b]; Chazdon, R[c]; Nelson, B. W.[d;] Cesar, R[a]; Meli, P.[a]; Gorgens, E. B.[e]; Duarte, M. M.[a]; Valbuena, R.[f,g]; Moreno, V. S.[a]; Mendes, A. F.[a]; Amazonas, N.[a]; Gonçalves, N. B.[d]; Silva, C. A.[h]; Schietti, J.[d]; Brancalion, P. H. S.[a]

SUPPLEMENTARY MATERIAL

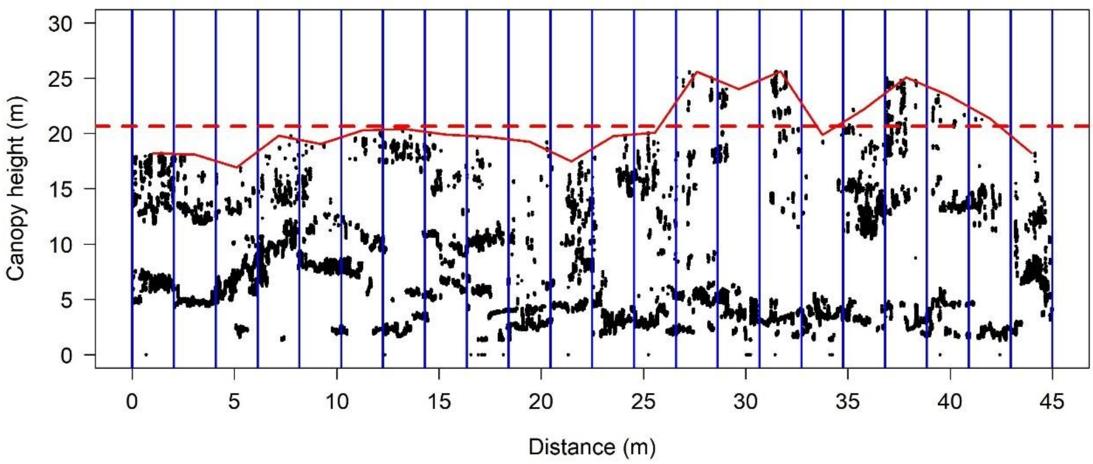

Figure S1- Example of a transect of PCL data (from an Old-growth forest), showingdivision of data into columns two meters long (vertical blue lines), the maximum points in each column (red solid line) and its average (red dashed horizontal line), which corresponds to canopy height attribute. The canopy rugosity attribute is the standard deviation of the maximum points. The attribute of canopy openness is the fraction of columns where the maximum point is less than 10 meters in height. In this example, since there are no columns with a maximum height lower than the 10-meter threshold, the canopy opening fraction is equal to zero (0/22 columns).

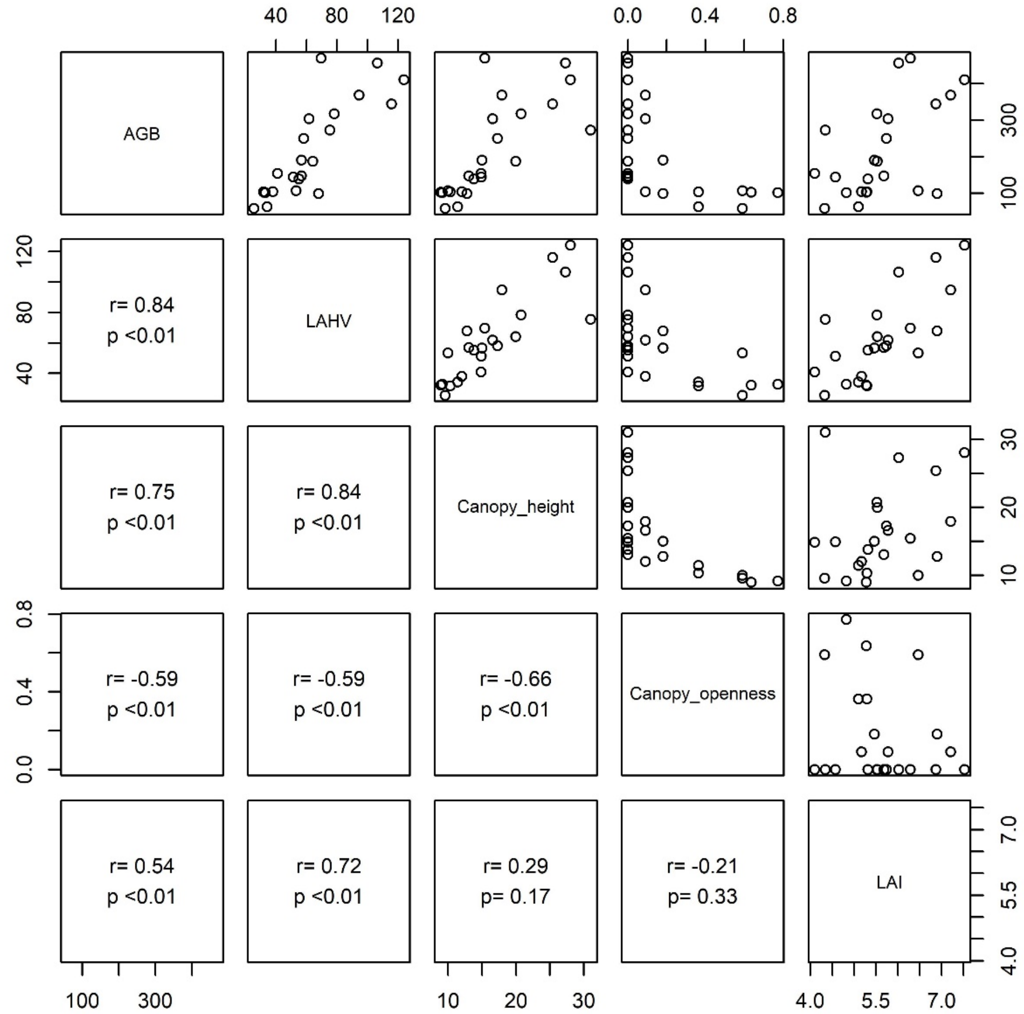

Figure S2 – Correlogram between AGB and the structural attributes of the canopy (derived from Lidar) at the Corumbataí study area with "Old-growth", "SGeuc" and "SGpas" typologies, using Pearson correlation.

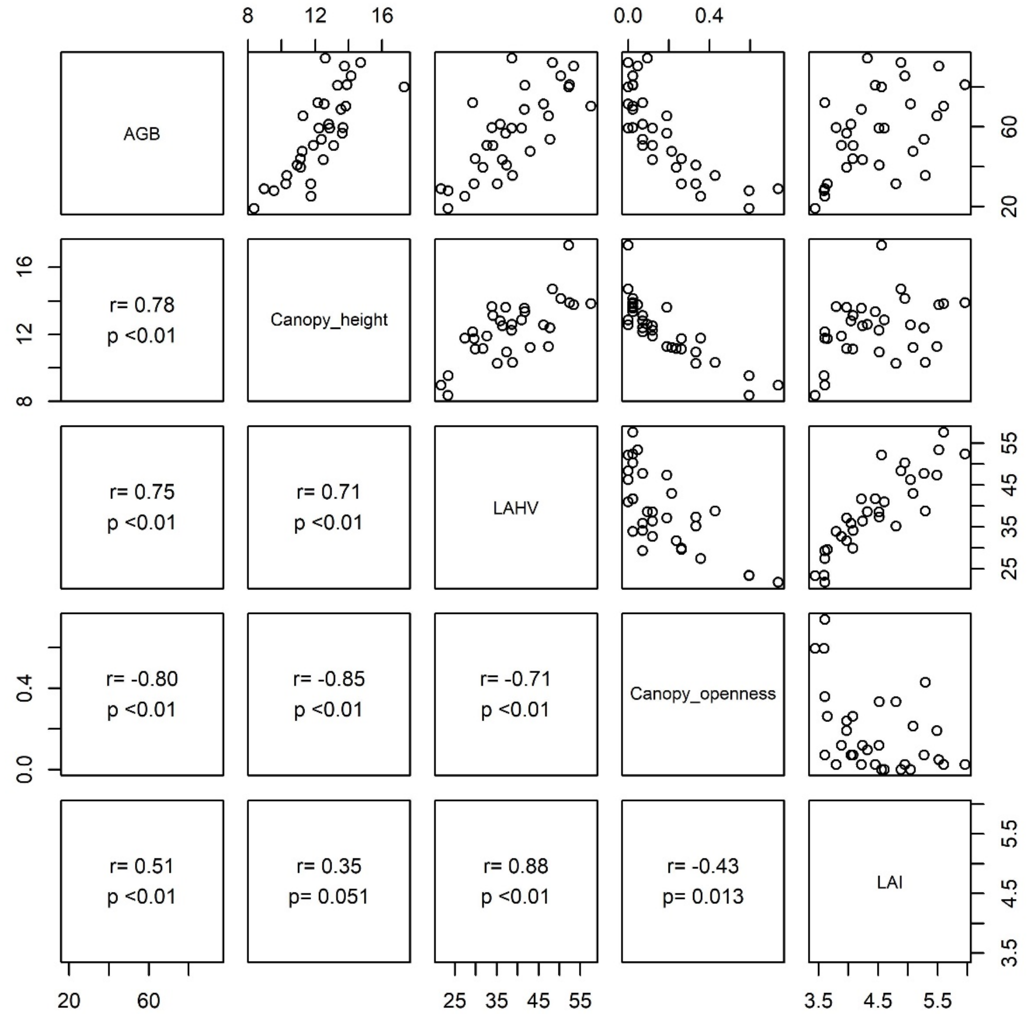

Figure S3 – Correlogram between AGB and the structural attributes of the canopy (derived from the Lidar) in the forest restoration plantation with biomass gradient, using the Pearson correlation.

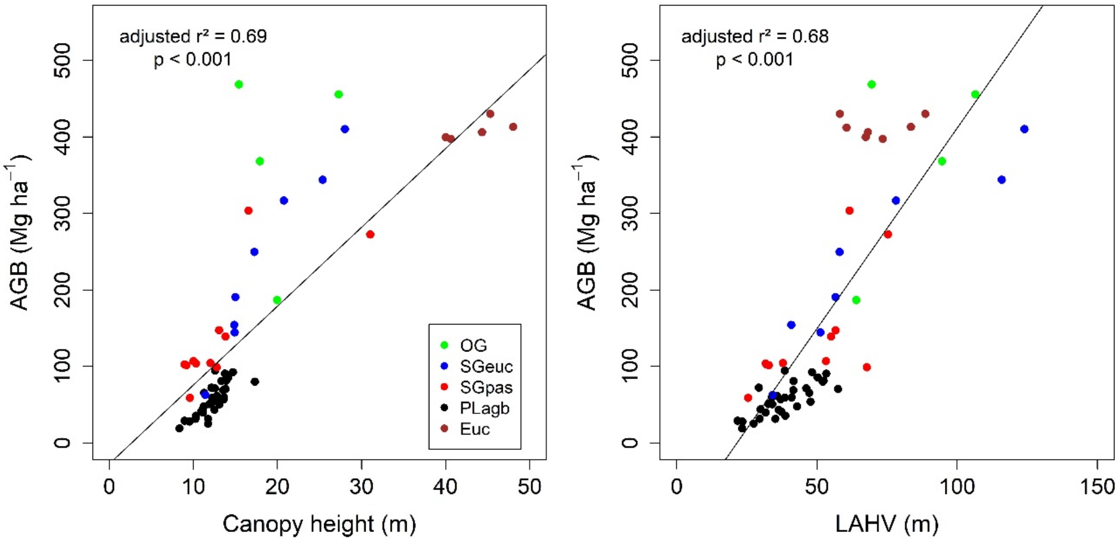

Figure S4. Aboveground biomass as a function of Canopy height (left) ($r^2 = 0.69$, RMSE = 80.31, relative RMSE = 51.9%); and as a function of LAHV (right) ($r^2 = 0.68$, RMSE = 80.9, relative RMSE = 52.3%).

Absolute and relative Root Mean Square Error (RMSE) were computed according to the equation below:

$$RMSE\ (Mg{\cdot}ha^{-1}) = \sqrt{\sum_{i=1}^{n}\left(y_i - \hat{y}_i\right)^2/n} \qquad \text{(Eq.S1)}$$

$$RMSE\ \ (\%) = 100 * \frac{RMSE\ (Mg{\cdot}ha^{-1})}{\overline{y}} \qquad \text{(Eq.S2)}$$

Where n is the number of observations, y_i is the observed aboveground biomass for plot i, $\hat{y}_i$ is the predicted aboveground biomass for plot i and $\overline{y}$ is the average of the observed aboveground biomass values.

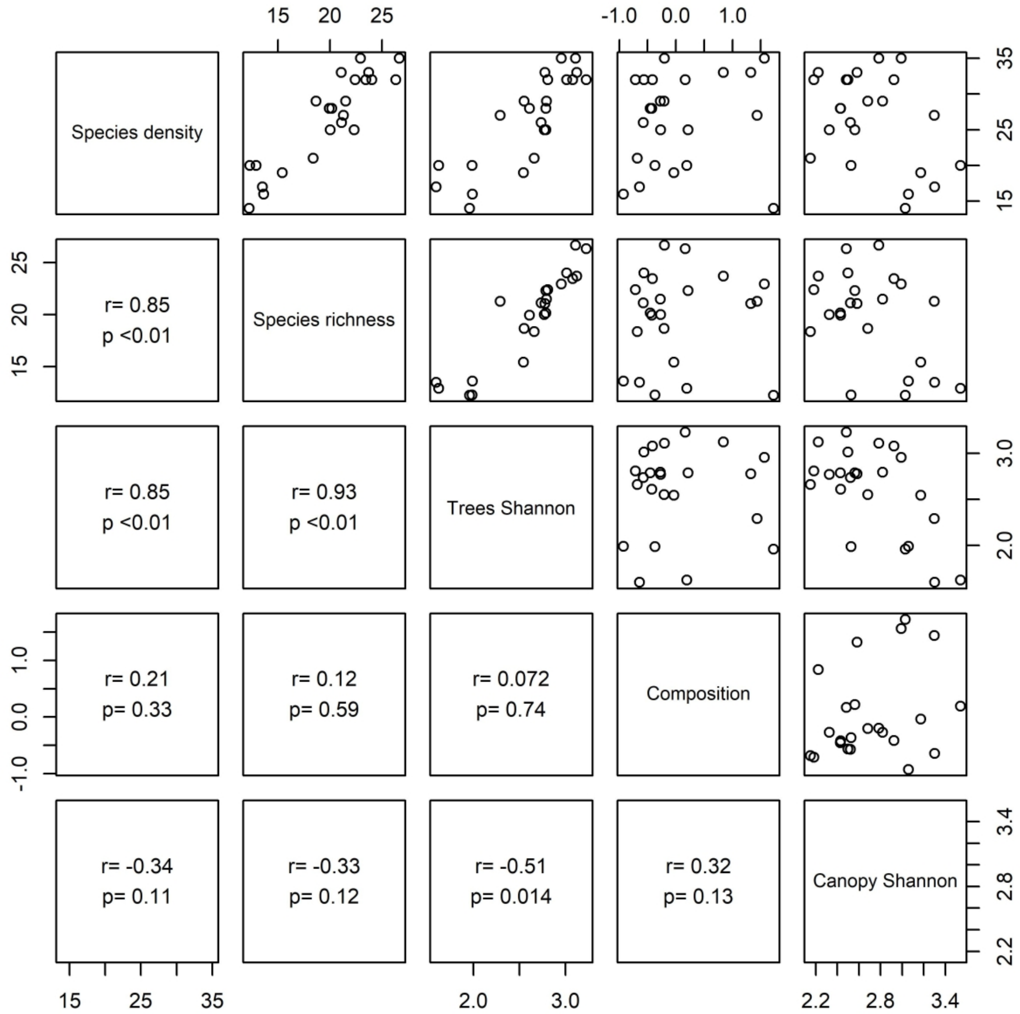

Figure S5 - Correlation between the tree species diversity variables (Species density, Richness, Shannon index and composition dissimilarity) and the structural attribute Canopy Shannon index (Lidar-derived) in the Corumbataí study area with the "Old-growth", "SGeuc" and "SGpas" using the Spearman correlation.

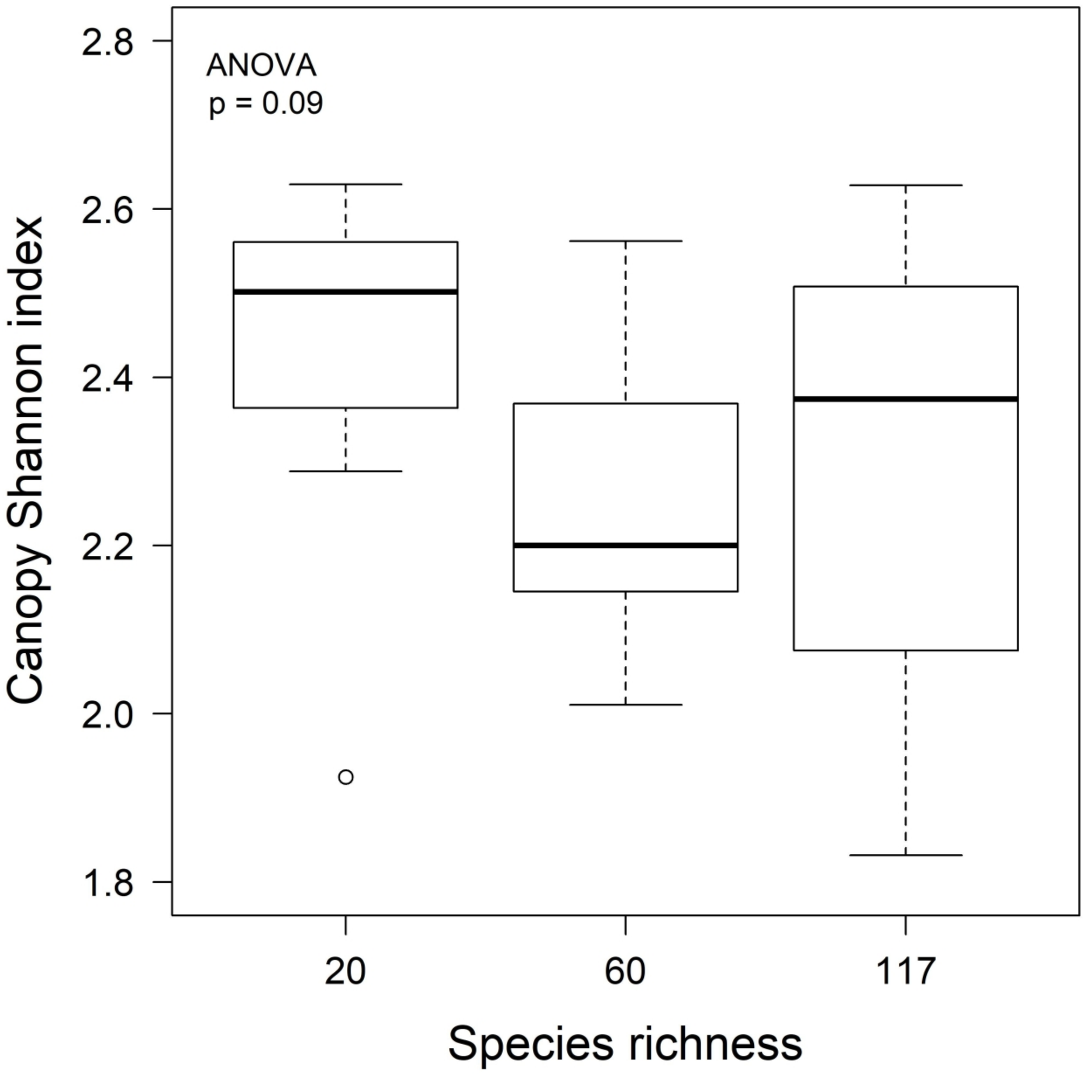

Figure S6 – Canopy Shannon index for different richness levels in the restoration plantation with species richness gradient (“PLdiv” tree cover type).

Table S1. Main attributes for each plot

Cover type	BA	AGB	Sps density	Richness	Shannon trees	NMDS	Canopy height	Openness	Rugosity	LAI	LAI_under	Shannon canopy	LAHV
OG	44,98	469	33	21	2,78	1,33	15,4	0,00	1,7	6,3	0,7	2,58	69,5
OG	25,98	187	14	12	1,96	1,73	20,0	0,00	4,7	5,5	1,1	3,03	64,1
OG	41,64	368	35	23	2,96	1,56	17,9	0,09	4,5	7,2	0,8	2,99	94,6
OG	43,25	456	27	21	2,29	1,44	27,3	0,00	2,8	6,0	0,8	3,30	106,6
SGeuc	8,82	63	28	20	2,61	-0,42	11,4	0,36	3,3	5,1	2,0	2,43	34,2
SGeuc	17,47	144	25	22	2,79	0,22	14,9	0,00	2,2	4,6	0,4	2,56	51,3
SGeuc	32,15	344	17	13	1,60	-0,64	25,4	0,00	6,4	6,9	0,9	3,30	116,0
SGeuc	31,67	317	19	15	2,55	-0,03	20,8	0,00	6,0	5,5	0,5	3,17	78,2
SGeuc	22,50	154	20	12	1,99	-0,37	14,9	0,00	1,1	4,1	0,8	2,53	40,9
SGeuc	38,06	410	16	14	1,99	-0,93	28,0	0,00	7,9	7,5	2,5	3,06	124,1
SGeuc	24,70	191	35	27	3,11	-0,20	15,0	0,18	4,7	5,5	0,7	2,78	56,7
SGeuc	24,29	249	32	23	3,08	-0,42	17,3	0,00	3,9	5,7	1,3	2,92	58,1
SGpasture	17,67	99	29	19	2,55	-0,21	12,8	0,18	3,1	6,9	1,3	2,68	67,8
SGpasture	30,45	272	20	13	1,62	0,19	31,0	0,00	9,0	4,3	0,6	3,54	75,4
SGpasture	15,30	104	32	26	3,23	0,17	12,0	0,09	1,5	5,2	1,5	2,49	37,9
SGpasture	17,21	104	25	20	2,77	-0,27	10,3	0,36	2,8	5,3	2,3	2,33	31,7
SGpasture	17,20	107	26	21	2,74	-0,57	10,0	0,59	3,8	6,5	1,0	2,52	53,2
SGpasture	26,08	304	29	21	2,79	-0,27	16,6	0,09	3,1	5,8	1,2	2,82	61,7
SGpasture	15,12	102	33	24	3,13	0,84	9,0	0,64	2,4	5,3	2,2	2,22	32,1
SGpasture	15,58	147	28	20	2,79	-0,45	13,1	0,00	1,3	5,7	0,5	2,43	56,7
SGpasture	17,22	139	32	24	3,02	-0,56	13,8	0,00	1,0	5,3	0,6	2,50	55,1
SGpasture	13,31	101	32	22	2,81	-0,71	9,2	0,77	1,5	4,8	1,2	2,18	32,8
SGpasture	8,22	59	21	18	2,66	-0,68	9,6	0,59	4,7	4,3	1,7	2,15	25,5
Euc	42,58	406	1	1	NA	NA	44,3	0,00	1,9	2,3	0,1	3,30	68,2
Euc	45,20	430	1	1	NA	NA	45,3	0,00	2,5	1,7	0,0	3,49	58,2

Euc	41,26	413	1	1	NA	NA	48,1	0,00	1,3	2,5	0,1	3,42	83,6
Euc	35,84	412	1	1	NA	NA	53,3	0,00	2,6	2,0	0,0	3,54	60,6
Euc	36,52	430	1	1	NA	NA	53,7	0,00	2,3	2,7	0,0	3,68	88,7
Euc	39,52	397	1	1	NA	NA	40,6	0,00	1,7	2,4	0,0	3,17	73,5
Euc	40,36	400	1	1	NA	NA	40,0	0,00	1,4	2,4	0,0	3,34	67,4
PLdiv	39,77	98	20	20	NA	NA	11,3	0,17	1,0	0,9	0,5	2,18	10,5
PLdiv	29,48	84	20	20	NA	NA	9,7	0,60	1,1	5,3	0,3	2,12	13,6
PLdiv	21,63	58	20	20	NA	NA	8,7	0,85	1,2	3,1	0,4	2,31	14,1
PLdiv	26,63	84	20	20	NA	NA	11,8	0,22	1,4	5,0	0,9	2,37	46,9
PLdiv	29,16	82	60	60	NA	NA	11,1	0,28	1,7	2,2	0,6	2,30	57,1
PLdiv	29,69	93	60	60	NA	NA	13,0	0,13	2,7	7,0	0,9	2,23	50,7
PLdiv	28,62	98	60	60	NA	NA	13,8	0,10	2,5	7,0	1,0	2,38	50,6
PLdiv	29,78	101	60	60	NA	NA	14,5	0,05	2,8	5,6	0,7	2,33	40,5
PLdiv	26,04	88	117	117	NA	NA	10,5	0,37	1,9	2,2	0,7	2,34	57,1
PLdiv	27,74	87	117	117	NA	NA	11,0	0,33	1,5	5,5	0,6	2,50	46,3
PLdiv	29,64	103	117	117	NA	NA	12,2	0,20	2,5	5,8	0,7	2,42	45,0
PLdiv	27,24	92	117	117	NA	NA	13,4	0,12	2,6	4,5	0,7	2,47	44,9
PLagb	33,15	92	20	20	NA	NA	14,7	0,00	1,0	4,9	0,9	2,57	48,3
PLagb	26,66	90	20	20	NA	NA	13,8	0,05	1,6	5,5	0,9	2,59	53,4
PLagb	16,86	41	20	20	NA	NA	10,9	0,33	1,5	4,5	0,7	2,26	37,3
PLagb	22,96	69	20	20	NA	NA	13,6	0,02	1,3	4,2	0,6	2,45	41,6
PLagb	21,61	59	20	20	NA	NA	12,2	0,12	1,8	4,5	0,7	2,44	38,5
PLagb	23,28	81	20	20	NA	NA	13,3	0,02	1,0	4,5	0,6	2,42	41,7
PLagb	16,44	40	20	20	NA	NA	11,1	0,24	1,7	4,0	1,0	2,35	31,7
PLagb	26,18	81	20	20	NA	NA	13,9	0,02	1,7	6,0	1,5	2,61	52,4
PLagb	23,91	54	20	20	NA	NA	12,4	0,07	1,3	5,3	0,7	2,31	47,7
PLagb	27,66	94	20	20	NA	NA	12,6	0,10	1,7	4,3	0,8	2,47	38,6
PLagb	12,72	28	20	20	NA	NA	9,5	0,60	1,4	3,6	1,1	2,17	23,4

PLagb	17,78	51	20	20	NA	NA	13,1	0,07	3,3	4,1	0,9	2,41	34,1
PLagb	18,00	44	20	20	NA	NA	11,1	0,26	3,0	4,1	0,9	NA	29,9
PLagb	25,18	71	20	20	NA	NA	12,6	0,00	1,1	5,0	0,5	2,40	46,2
PLagb	12,72	31	20	20	NA	NA	10,3	0,33	1,7	4,8	1,4	2,30	35,2
PLagb	21,69	61	20	20	NA	NA	12,8	0,07	2,1	4,0	1,0	2,40	35,8
PLagb	20,53	59	20	20	NA	NA	12,9	0,00	1,3	4,6	0,7	2,42	41,0
PLagb	24,30	70	20	20	NA	NA	13,8	0,02	2,1	5,6	0,6	2,51	57,6
PLagb	15,15	36	20	20	NA	NA	10,3	0,43	2,2	5,3	1,3	2,38	38,7
PLagb	17,98	43	20	20	NA	NA	12,5	0,12	2,9	4,2	0,9	2,44	36,4
PLagb	15,91	31	20	20	NA	NA	11,7	0,26	4,1	3,6	0,7	2,35	29,6
PLagb	29,42	86	20	20	NA	NA	14,2	0,02	1,4	5,0	0,6	2,53	50,3
PLagb	9,75	19	20	20	NA	NA	8,4	0,60	3,3	3,4	1,3	2,27	23,3
PLagb	18,59	72	20	20	NA	NA	12,2	0,07	1,5	3,6	0,9	2,47	29,3
PLagb	24,97	80	20	20	NA	NA	17,3	0,00	4,2	4,6	0,3	2,82	52,2
PLagb	22,27	65	20	20	NA	NA	11,3	0,19	1,4	5,5	0,8	2,26	47,3
PLagb	10,06	25	20	20	NA	NA	11,8	0,36	4,7	3,6	0,7	2,37	27,4
PLagb	20,23	48	20	20	NA	NA	11,2	0,21	1,5	5,1	0,8	2,35	43,0
PLagb	19,43	57	20	20	NA	NA	13,6	0,19	4,5	4,0	0,8	2,55	37,1
PLagb	18,36	51	20	20	NA	NA	11,9	0,12	2,7	3,9	0,9	2,50	32,7
PLagb	10,09	29	20	20	NA	NA	9,0	0,74	1,9	3,6	1,5	2,21	21,7
PLagb	20,65	60	20	20	NA	NA	13,7	0,02	3,2	3,8	0,8	2,47	33,9